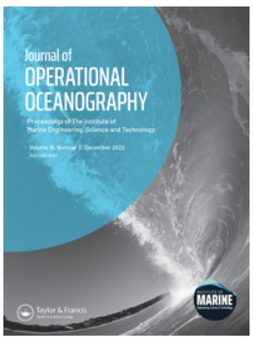

Journal of Operational Oceanography

ISSN: (Print) (Online) Journal homepage: https://www.tandfonline.com/loi/tjoo20

Swell and wind-sea partitioning of HF radar directional spectra

Lucy R. Wyatt & J. J. Green

To cite this article: Lucy R. Wyatt & J. J. Green (2022): Swell and wind-sea partitioning of HF radar directional spectra, Journal of Operational Oceanography, DOI: 10.1080/1755876X.2022.2127232

To link to this article: https://doi.org/10.1080/1755876X.2022.2127232

Published online: 28 Sep 2022.

JOURNAL OF OPERATIONAL OCEANOGRAPHY
https://doi.org/10.1080/1755876X.2022.2127232

Taylor & Francis
Taylor & Francis Group

Swell and wind-sea partitioning of HF radar directional spectra

Lucy R. Wyatt [a,b] and J. J. Green [a]

[a]Seaview Sensing Ltd, Sheffield, UK; [b]School of Mathematics and Statistics, University of Sheffield, Sheffield, UK

ABSTRACT

Partitioning is a process used to separate wind-sea and swell contributions in an ocean wave directional spectrum to simplify, and hence make more useful, the interpretation of the spectrum for users of wave data. HF radar systems can measure the wave spectrum over regions of the coastal ocean from the coast to over 100 km offshore with good spatial and temporal resolution depending on the operating frequency and bandwidth. Such systems can measure hundreds of directional spectra across the field of view of the radar, so there is very strong motivation to reduce the dimensionality of the data set for practical applications using partitioning. For similar reasons partitioning methods are increasingly being used for wave model and satellite-measured spectra. A partitioning method, which extends the method of Waters J, Wyatt LR, Wolf J, Hines A. [2013. Data assimilation of partitioned HF radar wave data into Wavewatch III. Ocean Model. 72:17–31.] for HF radar data, is described, assessed using buoy data and used to demonstrate the spatial variability of both swell and wind waves in three coastal regions. The results are very encouraging. HF radar systems could therefore provide very useful data for wave model and satellite partitioning validations in coastal waters where model and satellite measurements are most challenged by wave-current interactions, coastal topography and bathymetry.

ARTICLE HISTORY
Received 19 April 2021
Accepted 25 August 2022

1. Introduction

High-frequency (HF) radar systems, sometimes referred to as coastal radars, are normally located on the coast monitoring the ocean surface from the coast to a range that depends on radar operating frequency. They form part of a number of international operational oceanography networks (Fujii et al. 2013; Rubio et al. 2017; Harlan et al. 2010), providing surface current measurements for many scientific and operational activities. There is increasing interest in their use for wave and wind measurement although these are not yet routinely available from most systems. Metocean measurements are made from the power spectrum of the backscattered radio signal at HF frequencies (3–30 MHz). For most such measurements, greater accuracy and more detailed measurements are possible if the data from two radars looking at the sea from different directions are used. Measurements are often made on a spatial grid, the size and resolution of which depend on the radar operating frequency and bandwidth. HF radars are generally either phased-array radars that can measure backscatter from all positions on the defined spatial grid, or direction-finding radars which measure backscatter from annular rings centred on each radar location. The phased array configuration makes it much easier to make directional spectrum measurements and, in this paper, data from two such radars is used. These are the German WERA radar (Gurgel et al. 1999) and the UK Pisces radar (Wyatt et al. 2006). These differ in their signal modulation and thus the maximum power that can be used and hence range that can be achieved for a given radio frequency. The data were obtained from three high-energy sites, two in the Celtic Sea to the South West of Great Britain, exposed to the Atlantic to the south-west, WERA in the south and Pisces in the north, and the third a WERA on the North Atlantic coast of Norway. In all three cases, directional wave-buoys were deployed to validate the radar wave measurements.

The directional spectrum is a measure of the distribution of wave energy by wavenumber (or frequency) and direction. It contains information about locally generated wind waves and contributions from wind-generated waves propagating into the region from

CONTACT Lucy R. Wyatt lucywyatt@seaviewsensing.com, l.wyatt@sheffield.ac.uk Seaview Sensing Ltd, Sheffield, UK; School of Mathematics and Statistics, University of Sheffield, Sheffield, S10 2TN, UK

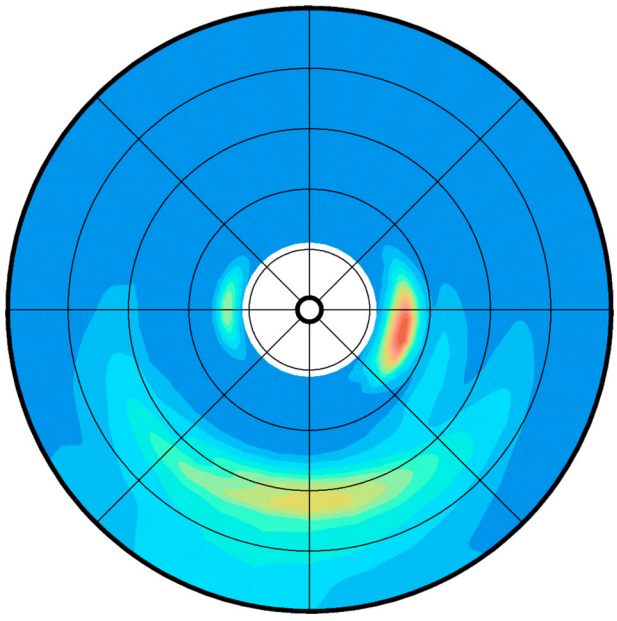

Figure 1. Directional spectrum measured with the University of Plymouth WERA radar on 28/11/2012@23:05. Circles are at frequency intervals of 0.05 Hz with an upper frequency of 0.25 Hz. The spectrum has been normalised by its maximum energy and the magnitude scale is linear from blue to red. Image obtained from an interactive metocean mapping facility for this deployment is available on the Seaview Sensing website (www.seaviewsensing.com, accessed April 6 2021).

distant storms, i.e. swell. Depending on the location and meteorological conditions, there could be a number of swell components. Figure 1 presents an example of a radar-measured directional spectrum plotted in polar form showing two low-frequency peaks (less than 0.1 Hz), which might be interpreted as swell the larger one propagating to the east, and wind waves with a peak at about 0.15 Hz propagating to the south. Spectra with swell and wind wave components are referred to as bi- or multi-modal.

The information contained within a spectrum is often summarised with a number of parameters derived from the spectrum such as significant waveheight, which measures the total energy in the spectrum, peak period and direction. In Figure 1, peak period and direction are roughly 0.07 Hz and 100°, respectively. If the wind were blowing a little more strongly, the peak direction could have been 170° since this was the wind direction at that location. Figure 2 shows peak direction and period across the measurement region of the University of Plymouth WERA radar. Figure 1 showed the spectrum at one position in this map which is marked with a white square towards the northwest of the map. This location is shown on subsequent maps with a green circle. It is clear that at some locations, including the one shown in Figure 1, the peak (shown in orange) is in the swell propagating towards the east and not the wind sea (shown in blue). Significant waveheight was fairly uniform across the coverage area at 1.75 m with a standard deviation of 0.22 m.

For some applications, e.g. ship safety, coastal erosion, some offshore engineering operations, model and satellite validation, it is important to know whether a spectrum is bimodal and to have separate amplitude, period and direction parameters for the wind-sea and any swell components. The process of automatically separating a spectrum into wind sea and swell is referred to as partitioning and is now a feature of many operational models. A number of different partition methods have been suggested (see Waters 2010 for a review). In some cases, these are applied to the 1D spectrum which is the integral of the directional spectrum over angle (Voorrips et al. 1997; Portilla et al. 2009). Of more relevance to HF radar measured wave spectra are methods that can be applied to 2D spectra such as Hasselmann et al. (1996), Hanson and Phillips (2004), Portilla et al. (2009). In some applications, wind speed has been used in a wave age criterion in order to identify the wind wave partition as part of this process (van Vledder and Akpinar 2016). In this paper, we present an extension of the method of Waters et al. (2013) applied to a number of different data sets in order to test the robustness of the approach, i.e can it be applied across the field of view of the radar system to produce sensible maps of swell and wind sea and can it be applied over time producing results similar to wave buoy measurements. The (Waters et al. 2013) method was developed for HF radar, buoy and model spectra and the partitions were used for data assimilation and validation. In order to do either of these, the same partitions need to be identified in all the measurement systems and the problems associated with this are discussed in that paper. We have not therefore attempted to partition the buoy measurements but instead use buoy parameters to give confidence in the partitioned parameters of the radar measurement. Our aim here is to show that partitioning of HF radar measured wave spectra provide information about the spatial variability in the wave field that would be very useful for users of wave data and that, therefore, could also be used to validate model and satellite partitioned spectra. We do not currently have a reliable wind speed measurement from the HF radar data so an alternative method to identify a wind wave partition is presented.

In Section 2, the method used to obtain the directional spectrum from the radar data is summarised. The partitioning method, and the extensions that we found were necessary to partition the data sets used

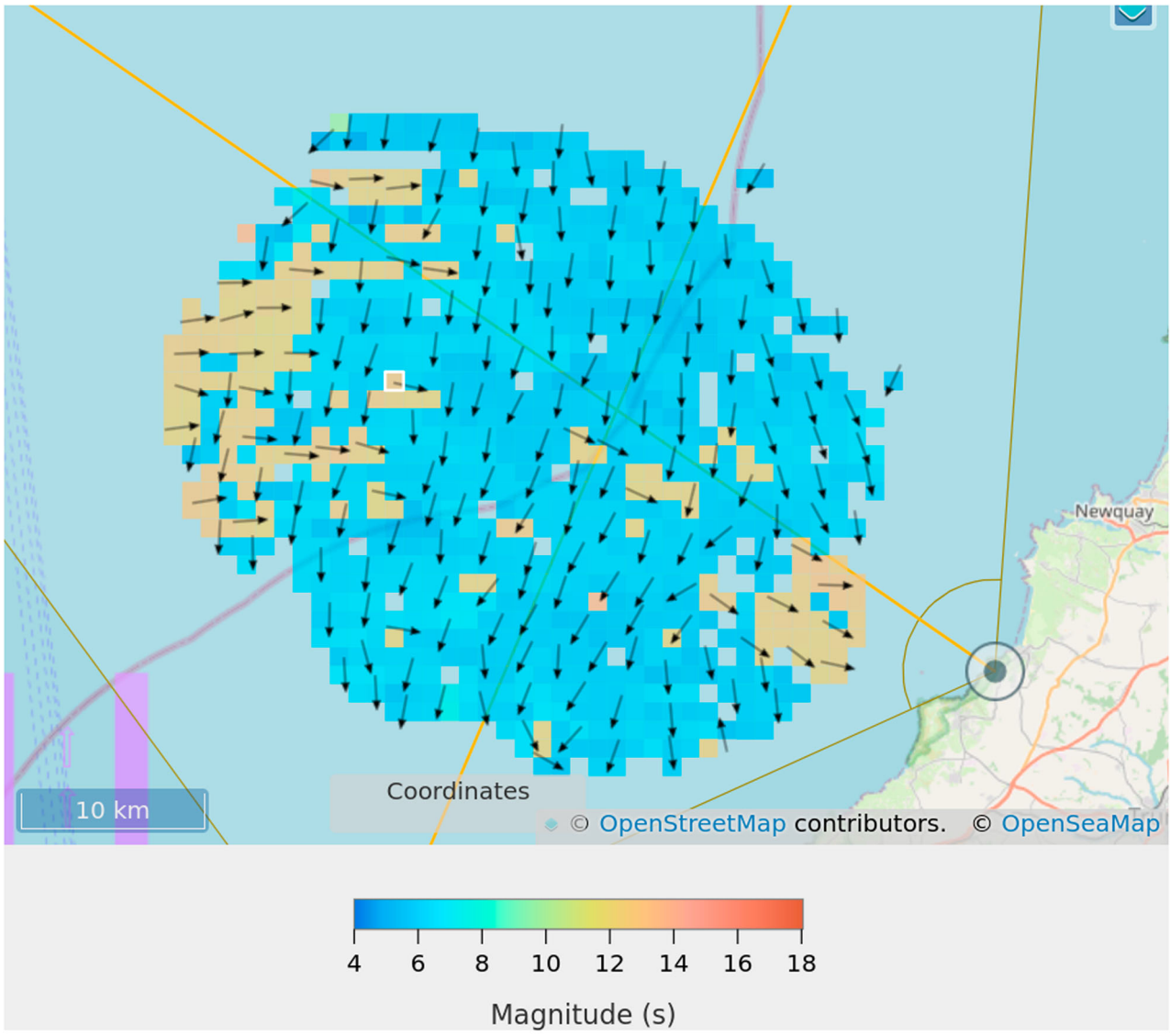

Figure 2. Peak period and direction measured with the University of Plymouth WERA radar (Lopez and Conley 2019) on 28/11/2012 at 23:05. One of the radar sites is indicated with ⊙. The white square marks the position of the spectrum in Figure 1. Image obtained from an interactive metocean mapping facility for this deployment available on the Seaview Sensing website (www.seaviewsensing.com, accessed 30 June 2022). When using the site, as the mouse moves over the image the word 'Coordinates' changes to the local longitude, latitude.

here, are presented in Section 3. Maps of the partitions and of those identified as swell and wind sea are shown in Section 4, which also includes a quantitative comparison with buoy data at one of the sites.

2. Obtaining the directional spectrum

The method used here to obtain the directional spectrum from the radar power spectrum is presented in Wyatt (1990), Green and Wyatt (2006). It is a numerical method that inverts the integral equation (Barrick 1972b; Lipa and Barrick 1986) relating the two types of spectra. The integral equation contains first- and second-order components associated with scattering from first- and second-order ocean wave components (Barrick 1972a 1972b; Barrick and Weber 1977). The second-order part of the spectrum contains the useful wave information and is normalised by the first-order part so that the method does not require any external calibration. The method is fast enough to allow for near real-time measurement of the directional spectrum and parameters derived from it at hundreds of locations across the field of view of the radar as shown in Figure 2.

These measurements can be made when there is sufficient signal-to-noise in the radar power spectrum and this depends on waveheight (Wyatt et al. 2011). It is also affected by radio interference and available power. Separating the first- and second-order

components in a measured spectrum is not always easy due to noise levels or to other sources of backscatter, e.g. ships or antenna sidelobes which can introduce some noise into the measured ocean wave directional spectrum at low frequencies. The separation process determines the lowest wavenumber (frequency) in the measured spectrum. If the signal is clean, the first-order spectrum consists of two clearly defined narrow peaks. The narrower and clearer the peaks, the lower the ocean wave frequency that can be measured.

The inversion solves for the directional spectrum for wavelengths down to a minimum(up to a maximum in wave frequency) that depends on the radio wavenumber and which varies with measurement position relative to the radar site. The upper limit in terms of wave frequency can be seen as a white line with red dots in Figure 3, which shows a directional spectrum (now as a function of direction (x-axis) and frequency (y-axis) measured with the University of Plymouth WERA radar which operates at about 12 MHz (Lopez and Conley 2019). Measurements at wave frequencies above this line are less well constrained by the inversion. A higher radio frequency is needed to measure shorter waves. In low wind conditions, all the wind wave energy will be at frequencies above the line. At this site there is usually swell and sufficient wind so measurements can be made at 12 MHz.

Parameters such as significant waveheight, H_s (shown in Figure 3), mean and peak period and direction are determined from the spectrum using standard methods (Hauser et al. 2005).

3. The partitioning method

The first stage of this process is similar to that described in Hasselmann et al. (1996), where the spectrum is described as an inverse catchment area or drainage basin wherein each drop of rain travels downward to a local minimum and all drop points with the same local minimum are in the same catchment or partition. This is achieved by creating a 'mask grid' the same size as the directional wavenumber spectrum grid. For each pixel on the mask grid, we move to an adjacent pixel in such a way that the corresponding directional spectrum value is maximised (there are at most eight adjacent pixels). If that mask pixel is 'marked' with a partition number, then we backtrack our path to the original pixel and mark all of that path with the same partition number. If not then we proceed in the same way. Eventually (by exhaustion) we meet a maximising pixel, in that case we create a new partition number there and backtrack as previously.

This produces a list of partitions which are then ordered by their significant waveheight. The spectrum obtained through the inversion can sometimes include noise and spurious peaks associated with ships or interference in the radar signal and these can generate spurious partitions and/or too much partitioning at this stage. Similar problems occur with partitioning of buoy or other data sources. A second stage is, therefore, usually required which involves the intelligent combining of partitions with the aim of clearly separating the spectrum into realistic wind-wave and swell components. The method used to combine partitions is based on that of Waters (2010), Waters et al. (2013), which was developed from those of Hasselmann et al. (1996) and Hanson and Phillips (2004) and involve the following steps.

(1) The first step is to identify and remove small (less than 5% of the sum of partition waveheights) partitions that have a peak or a centre of gravity that is greater than the inversion limit (the red and white line in Figure 3). These are poorly constrained by the inversion and, if retained, can introduce noise into the wind-wave classification.
(2) Determine (a) the distance between the peak of the largest partition (referred to as $P0$ below) and all other peaks, $\triangle k$, and (b) for all peaks, the spectral spread $\overline{\delta k^2}$ is defined as follows.

$$\begin{aligned}\overline{\delta k^2} &= \overline{(k_x - \overline{k_x})^2} + \overline{(k_y - \overline{k_y})^2} \\ &= \overline{k_x^2} - \overline{k_x}^2 + \overline{k_y^2} - \overline{k_y}^2\end{aligned}$$

where

$$\overline{k_x} = \frac{1}{e}\iint S(k,\,\theta)k\cos(\theta)\,\mathrm{d}\theta\,\mathrm{d}k$$

$$\overline{k_y} = \frac{1}{e}\iint S(k,\,\theta)k\sin(\theta)\,\mathrm{d}\theta\,\mathrm{d}k$$

$$\overline{k_x^2} = \frac{1}{e}\iint S(k,\,\theta)k^2\cos^2(\theta)\,\mathrm{d}\theta\,\mathrm{d}k$$

$$\overline{k_y^2} = \frac{1}{e}\iint S(k,\,\theta)k^2\sin^2(\theta)\,\mathrm{d}\theta\,\mathrm{d}k$$

Note that this is similar to the definition in Hanson and Phillips (2004) but at this point we are working with the wavenumber, k, spectrum, $S(k,\,\theta)$, rather than frequency.
(3) Order the remaining peaks by increasing distance $\triangle k$.
(4) For each peak in order in this list determine if it has a mutual boundary with $P0$ and if it does find the value of the spectrum at the boundary point,

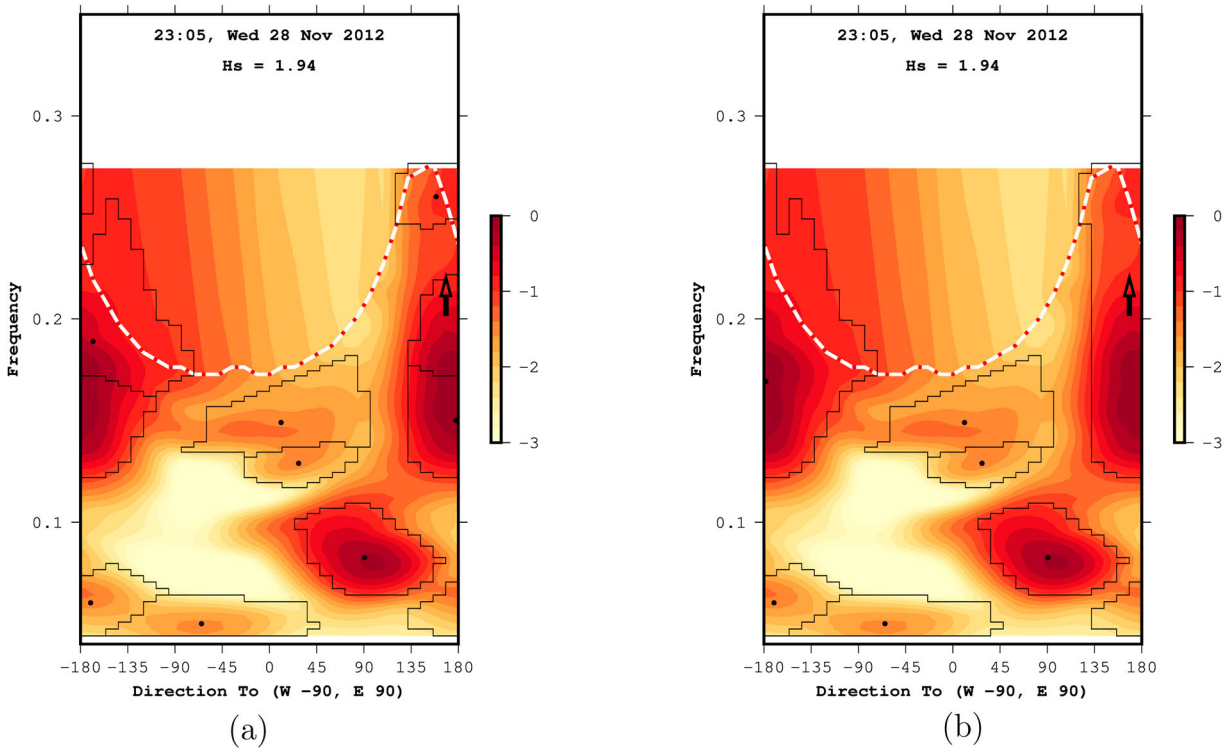

Figure 3. Directional spectrum measured with the University of Plymouth WERA radar on 28/11/2012 at 23:05 at position marked with a green square in Figure 4. (a) is the initial partitioning and (b) after combining partitions. The spectra have been normalised to the peak and amplitudes are plotted on a log scale as shown. The black lines mark the boundaries of the partitions. Black dots mark the centres of gravity of the partitions. The white-red line is the upper bound of the inversion. The black arrow is wind direction measured by the radar.

Smin, that lies between the two peaks. If a mutual boundary point is found continue otherwise go to the next partition in the list.

(5) For parameters A, B, C, D, if any of the following criteria are satisfied the two segments, $P0$, $P1$, will be merged.
- The peaks are too close i.e. $\triangle k$ is less than twice the wavenumber resolution
- The spread of either peak is larger than the square of the distance between them i.e. $B\overline{\delta k^2} > \triangle k^2$
- The trough between the peaks is not low enough. This involves two criteria and both have to be satisfied. $S_{\min} > A \min(P0, P1)$ and $S_{\min} - \min(P0, P1) < C \max(P0, P1)$. In these expressions min and max refer to the peak amplitudes in the partitions. The second criterion was not required in Hanson and Phillips (2004), Waters et al. (2013) but gives better results for the data sets we are using here.
- Both peak wavenumbers are greater than 0.8 times the maximum wavenumber in the inversion and their directions are within D° of the wind direction.

The constants A, B, C introduced here have been set at 0.7, 0.3, 0.1, respectively. The A and B values are the same as those used by Waters et al. (2013) for HF radar data. D has been set to 60°. Waters et al. (2013) and Hanson and Phillips (2004) found that different values were needed for model and buoy partitioning due to differences in the smoothness of the spectra.

(6) If conditions have been met, merge $P1$ with $P0$ to create a new $P0$ and calculate the spread, $\overline{\delta k^2}$, of the enlarged partition. Remove $P1$ from the ordered partition list.

(7) Repeat from (4) until the list is exhausted.

(8) Repeat from (2) where $P0$ is now the largest partition not yet merged.

(9) Order the partitions by wavenumber. If the highest wavenumber partition has a peak at wavenumber greater than 0.8 times the maximum wavenumber in the spectrum and this and the next highest both have a direction within D° of the wind direction, combine these segments and remove the smaller one. This combined segment is classified as the wind-wave segment. This step was not used in

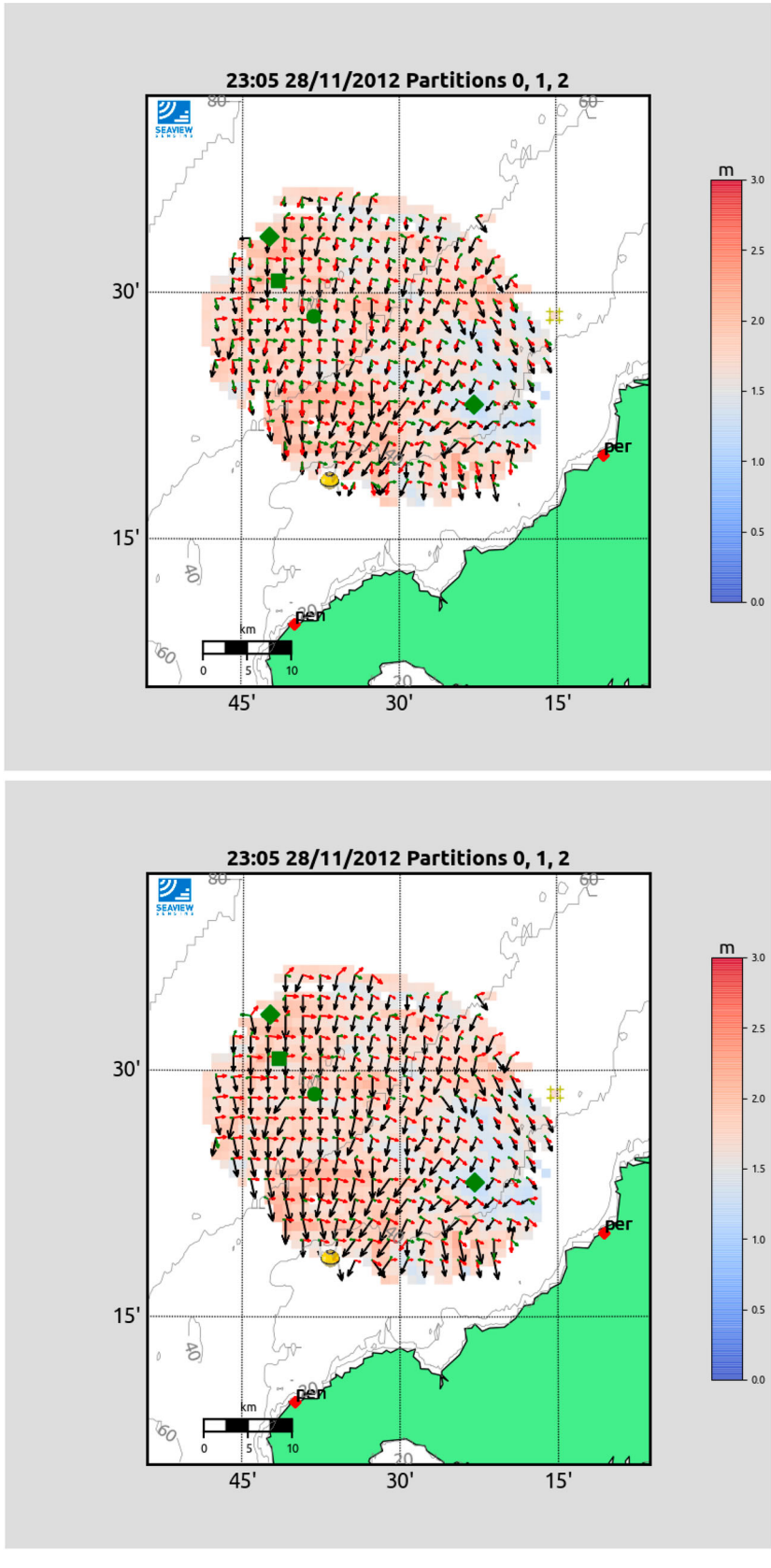

Figure 4. 28/11/2012 at 23:05 maps showing the directions and magnitude of largest three partitions as arrows, black largest, red second and green third. The total waveheight is colour-coded as shown. (a) is before partition combining, (b) is after. Water depth is contoured at 20 m increments. For clarity not all direction measurements are shown. The green symbols mark locations where plots of wave spectra have been included in this paper – see text for details. The location of the buoy used for validation is shown with a yellow buoy image. Radar sites at Penrith (pen) and Perranporth (per) marked with red diamonds.

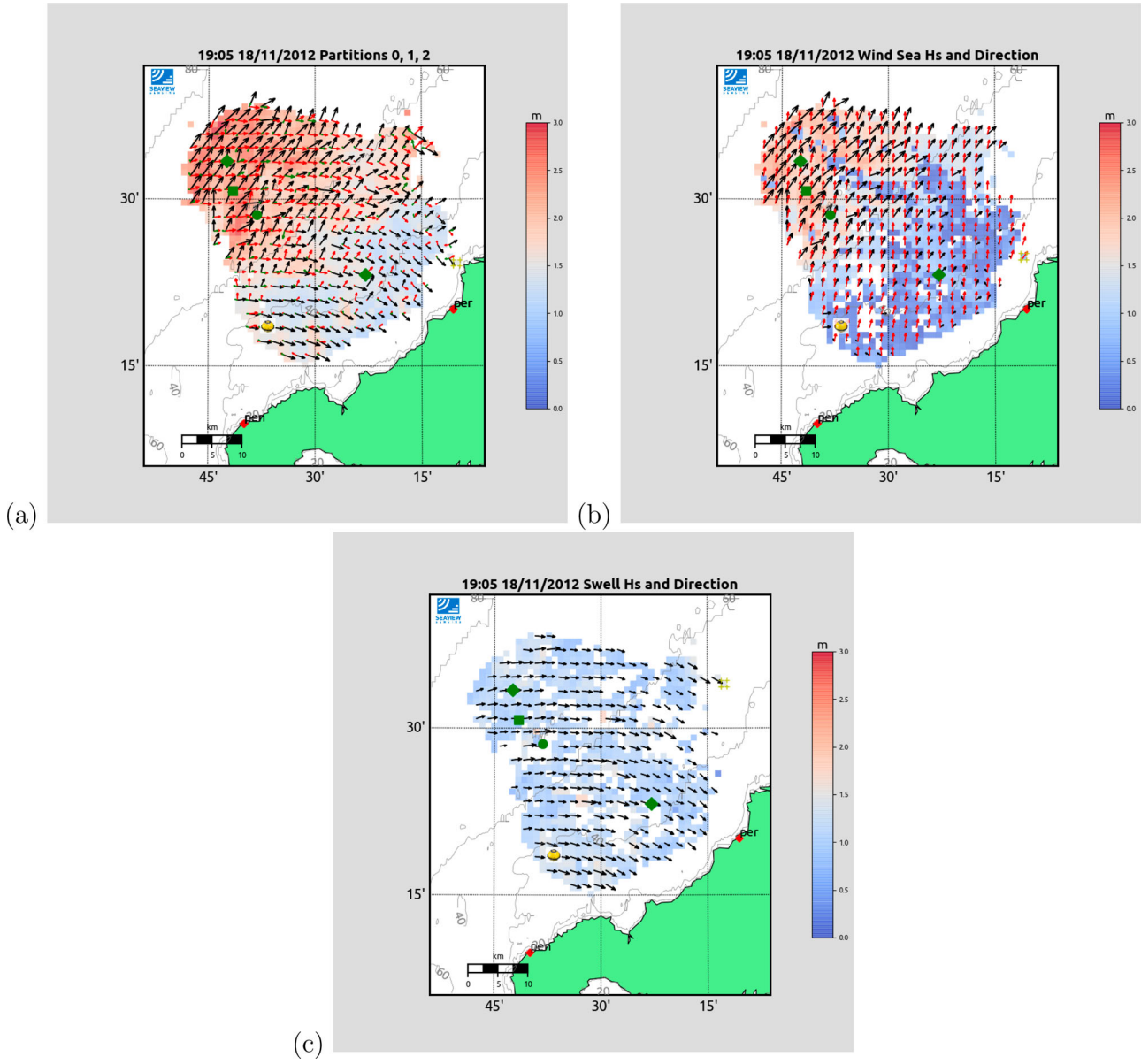

Figure 5. 18/11/2012 at 19:05 maps. (a) shows total waveheight and the directions and magnitudes of the largest three partitions as arrows, black largest, red second and yellow third. (b) show the wind wave partition magnitude (colour-coded and arrow length) and direction (black arrow) and wind direction (red arrow) and (c) shows the main swell partition. The associated waveheight is colour-coded as shown. Water depth is contoured at 20 m increments. For clarity not all direction measurements are shown. Green triangles mark the positions of the spectra shown in Figure 6. Radar sites at Penrith (pen) and Perranporth (per) marked with red diamonds.

Hanson and Phillips (2004), Waters et al. (2013), but it is needed for HF radar data, particularly if we want to identify the wind-sea partition, because the higher frequencies in the inversion are less constrained as discussed earlier so high-frequency partitioning is not as reliable.

(10) All partitions with peak wavenumber less than the wind wave partition (or all partitions if no wind-waves were found) are classified as swell. Some partitions may be unclassified.

(11) Waveheights and other parameters are calculated for the partitions that remain after this process and these are then ordered again by waveheight. Only the largest N (we have used $N = 5$) partitions are retained.

4. Results

Figure 3 shows partitions before and after combining. Although we limit the number of partitions to 5 normally, all identified partitions are shown in this figure so the process and the comparison can be seen more clearly. In this case, and for many of the measured spectra on this day and time, the original partitioning (a)

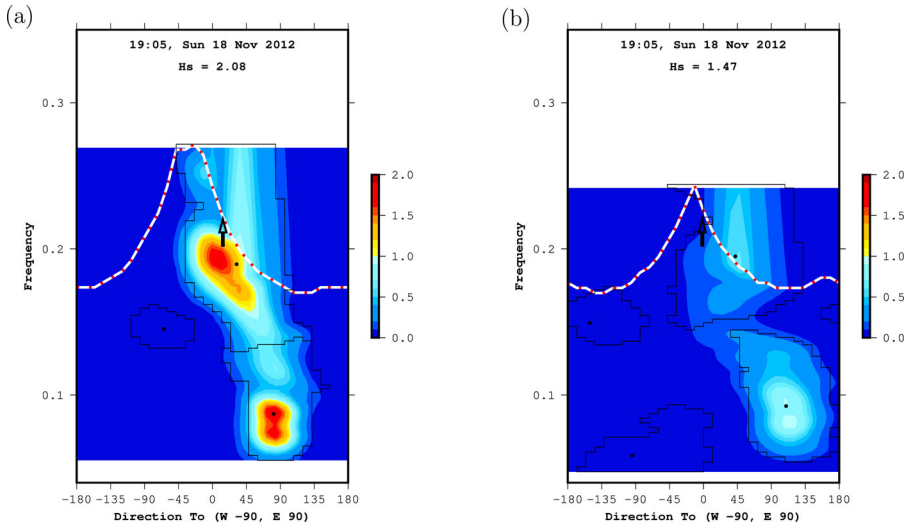

Figure 6. Directional spectra measured with the University of Plymouth WERA radar on 18/11/2012 at 19:05. The colour scale is linear in this case in units of m^2/Hz/radian. (a) is from an offshore cell and (b) one closer to the coast as indicated with green triangles in Figure 5. The black lines mark the boundaries of the partitions. Black dots mark the centres of gravity of the partitions. The white-red line is the upper bound of the inversion. The black arrow is wind direction measured by the radar.

split the main wind wave spectrum into three which were subsequently combined (b). The impact is clearer in Figure 4 where the directions and magnitudes of largest three partitions before (a) and after (b) combining are shown as arrows. In Figure 4(b), the largest partition (black) shows the wind-sea from the north and the second (red) partition shows swell from the west. This is less clear in (a) where the swell component is often the third largest. Note that there are two low-frequency partitions identified in these figures. These may be swell but could also be associated with noise as discussed earlier. In this and subsequent maps a yellow buoy image is used to show the position of buoys that have been used to validate the radar wave measurements.

Figure 5 shows data from 18/11/2012 at 19:05 when the radar measured wind blowing from the south as shown with red arrows in (b). Note that the signal-to-noise requirements for wind direction measurements are not as strict as that for waves hence there are more such measurements. The largest partition (black arrows on the left) has a different behaviour offshore than onshore. This is a case with fetch-limited wind waves and swell from the west as shown in (b) and (c), respectively. There are gaps in the wind wave partition close to the coast where the spectrum is dominated by swell and the classification is more subject to noise. As the fetch increases the wind sea waveheight increases as can be seen and becomes dominant further offshore. The offshore wind-waves are at more of an angle to the wind direction probably because this is a direction of longer fetch.

The swell partition shown in (c) is identified by first finding the median period and direction across the coverage area of the largest partition that was classified as swell. The map shows the swell partition at each location that has the minimum direction difference from the median of all swell partitions at that location with periods within 20% of the median period, where this difference is within 60° to allow for refraction in the shallower regions nearer the coast. There are a few gaps in the coverage where none of the swell partitions matched the selection criteria.

This example demonstrates very clearly the variability in the wave field in the coastal zone and thus the advantage of using an HF radar to make these measurements. Two partitioned spectra from this time are shown in Figure 6. The one from closer to the coast (b) is an example where the wind-wave part is only just picked up in the inversion and the swell is weaker.

Data from the University of Hamburg WERA radars operating at 27 MHz deployed on islands off the west coast of Norway during the EuroROSE project (Wyatt et al. 2003) are shown in Figure 7. The upper and lower figures are separated by 6 hours during which time the winds have changed from north easterly to south easterly. The swell from the north west dominates both these cases. Under winds from the north east (a, b), and thus fetch limited, the wind-sea coverage is rather patchy due to difficulty in the classification in these conditions because the wind-sea is at a frequency above the maximum measureable by the radar (as discussed in Section 2). When winds are from the south east (c, d), longer fetch and thus lower frequency wind waves propagating against the swell can be clearly identified.

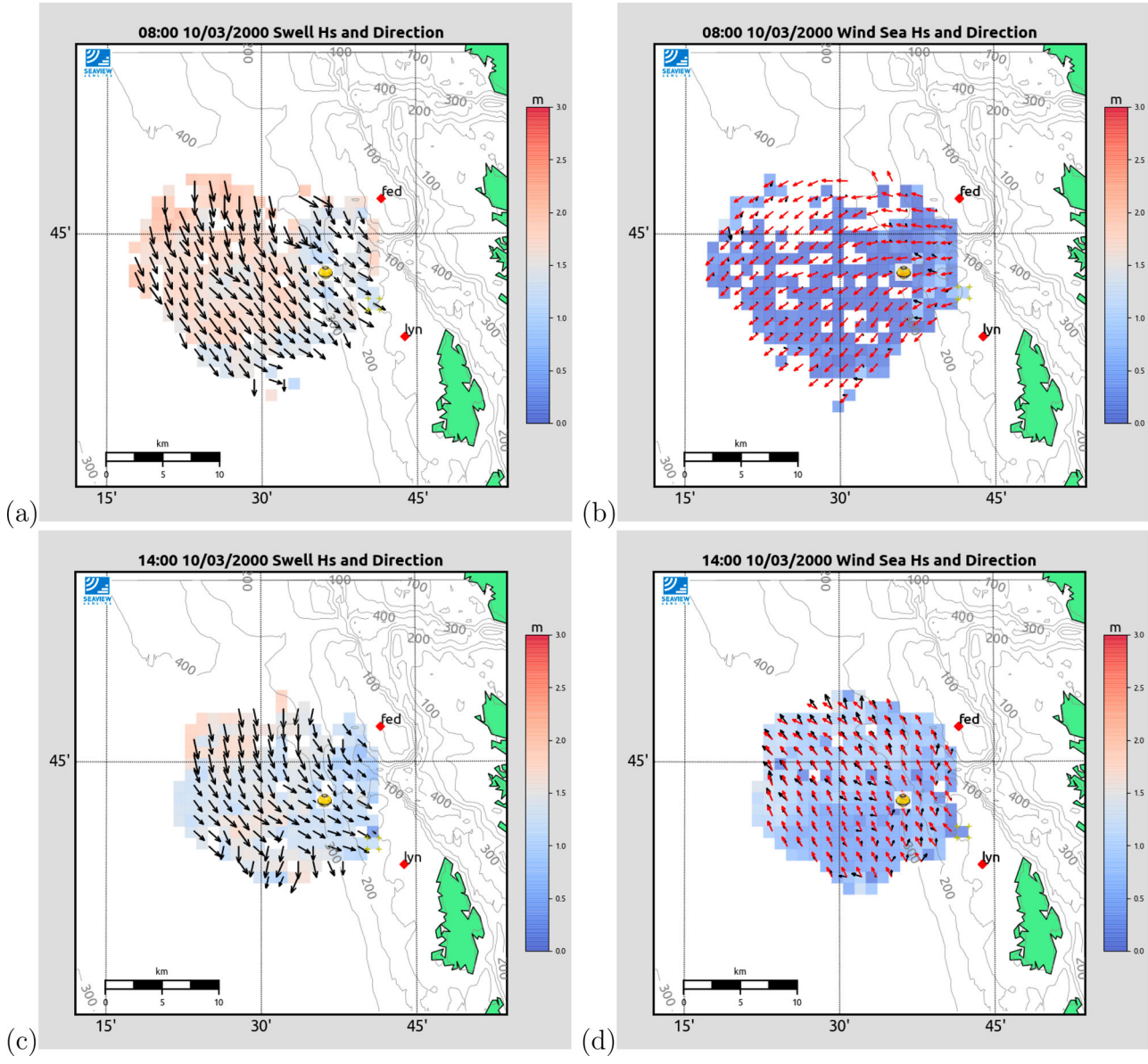

Figure 7. 10/03/2000 maps at 08:00 (a), (b) and at 14:00 (c), (d) using the University of Hamburg WERA. (a) and (c) show waveheight and direction of the largest swell partition. (b) and (d) show the wind wave partition magnitude (colour-coded and arrow length) and direction (black arrow) and wind direction (red arrow). The waveheight is colour-coded as shown. Depths are contoured at 100 m intervals. For clarity not all direction measurements are shown. Radar sites at Fedje (fed) and Lyngoy (lyn) marked with red diamonds.

The final example demonstrating the value of a spatial measurement of the wave field in coastal regions, Figure 8, shows just the wind wave partitions measured with a Neptune Radar Pisces system (Wyatt et al. 2006) at a time when a westerly wind (seen over the southern part of the region) had begun to veer to a more northerly direction in the north of the region. Waves generated by the westerly wind are clearly seen to the south and, in the north, wind waves from the north. The radar operating frequency, about 8 MHz in this case, was really too low for accurate measurement of the northerly wind waves so there are a couple of gaps. Pisces is now able to operate at more than one frequency providing more flexibility in different metocean conditions (Wyatt et al. 2019). Note that at the time of this measurement Pisces operated with limited spatial resolution.

The dataset from the University of Plymouth WERA is used to validate the peak frequency and direction of the largest partition. They are compared with the peak in the spectrum measured by a buoy located to the south-west of the radar coverage region (see Figure 5) and using the original implementation in Seaview software in Figure 9. The waveheight of the partition is also compared to the total waveheight showing that, at this position, most of the wave energy is associated with this partition

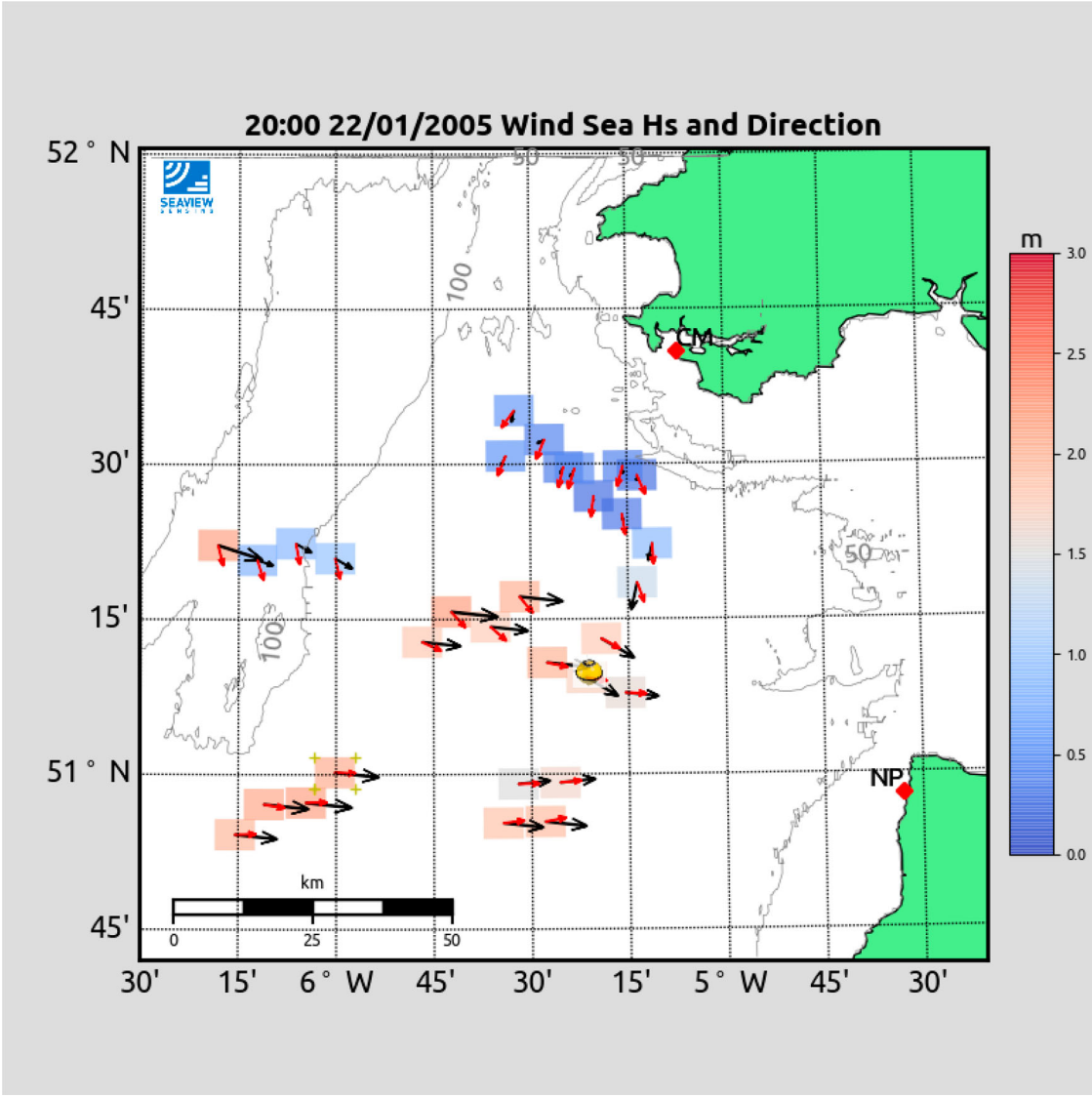

Figure 8. 22/01/2005 at 20:00 map of the wind sea component measured with the Pisces showing magnitude (colour-coded and arrow length) and direction (black arrow) and wind direction (red arrow). The waveheight is colour-coded as shown. Depths are contoured at 50 m intervals. Radar sites at Nabor Point (NP) and Castlemartin (CM) marked with red diamonds.

throughout this period. The peak period comparison with the buoy has a correlation coefficient of 0.77 and a scatter index of 0.18 and the peak direction comparison has a complex correlation of 0.92 and a mean difference of 5.0°. Note that we are not comparing exactly the same parameter here so some differences are expected. The buoy peak is the peak in the 1D frequency spectrum, the radar partition peak is the frequency corresponding to the peak in the 2D directional wavenumber spectrum.

5. Concluding remarks

We have demonstrated that wave spectra measured with HF radar, using different radar systems at different frequencies, can be partitioned in a robust and meaningful way providing clearer information for users about the sea surface conditions. Although we have not applied the same method to the buoy data used to assess the accuracy of the method, the peak partition period and direction show good agreement with the equivalent buoy spectral peak parameters for a period of more than one month of data from the University of Plymouth radar and better agreement than the standard Seaview peak parameter estimates which are more susceptible to noise in the radar data. Note that, as discussed in Waters et al. (2013), to apply the method to buoy data it would first have been necessary to estimate a directional spectrum from the more limited buoy spectral parameters. The spatial coverage provided by HF radar shows clear spatial variability in partition parameters on scales of a few kilometres emphasising the importance of such coverage in complex coastal environments and providing

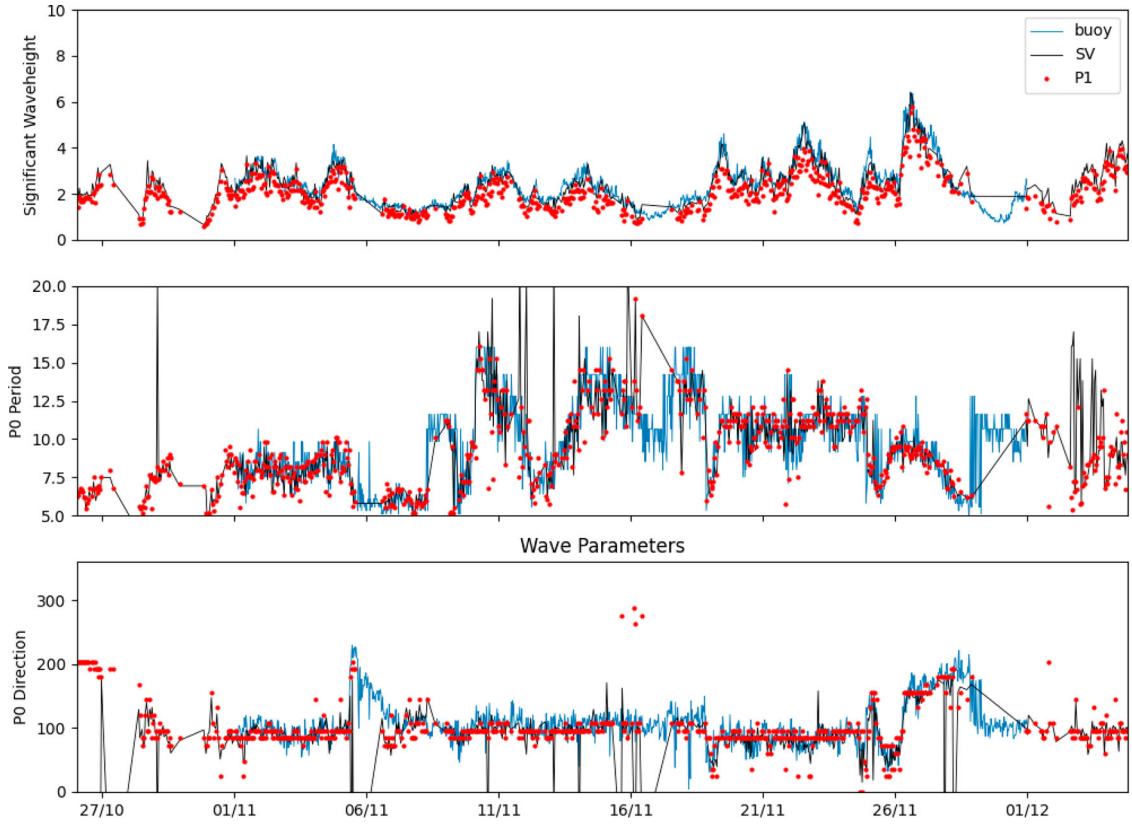

Figure 9. Wave parameter comparisons for the University of Plymouth WERA from the radar measurement cell that includes the location of the buoy marked with a yellow buoy image in Fig 5. Upper panel shows significant waveheight, middle panel peak period and lower panel peak direction. Blue line is the buoy measurement (buoy), black line the measurement using the original implementation in Seaview software (SV) and red dot is the corresponding parameter from the largest partition (P1).

opportunities for validation of wave model and satellite wave spectra partitioning.

The criteria used to identify the wind sea and main swell partitions presented here, although mostly appropriate for these data sets, are somewhat subjective and data-dependent. Some gaps can be seen in the coverage obtained for these due to this selection process. This is an area of ongoing research. A measure of spatial and possibly temporal continuity for individual spectral partitions may be helpful. In addition, such an approach should help to identify spurious partitions that are associated with noise, ships and antenna sidelobes in the radar data such as the low-frequency partitions seen in Figure 3 and the larger errors seen in the original Seaview timeseries, SV in Figure 9. These can then be removed from the spectrum increasing the accuracy of spectral parameters such as significant waveheight. Another reason for gaps in the data is the upper-frequency limit in HF radar wave measurement, which prevents wind-wave measurement in limited fetch geometries. This limit increases with radio frequency so an ability to use more than one radio frequency (Wyatt et al. 2019) will be advantageous.

Acknowledgement

The University of Plymouth radar and buoy data were provided by Daniel Conley with financial support from the Natural Environment Research Council [grant number NE/J004219/1]. The Norwegian data were obtained during the EU-funded EuroROSE project and provided by Klaus Werner Gurgel, University of Hamburg. The Pisces Celtic Sea data were provided by Neptune Radar and collected during a project funded by DEFRA and the Met Office.

Disclosure statement

Lucy Wyatt and Jim Green are founders and part-owners of Seaview Sensing Ltd. Both have a history of publications that demonstrate objective scientific research. The company may benefit from the research results presented here.

Funding

This work was funded by the University of Sheffield and Seaview Sensing Ltd.

Notes on contributors

Lucy R. Wyatt: BSc Mathematics, MSc Fluid Mechanics, PhD Physical Oceanography. Research experience at Johns

Hopkins University, USA, Reading and Birmingham Universities UK, ACORN Director James Cook University Australia. Lecturer, Senior Lecturer, Reader, Professor, Emeritus Professor University of Sheffield. Co-founder and Technical Director Seaview Sensing Ltd.

J. J. Green: Doctorate in Mathematics, researcher at the National Physical Laboratory, University of Sheffield, l'Observatoire de Paris; Currently Senior ML engineer at Dressipi, London; Co-founder, and Software Developer Seaview Sensing Ltd.

ORCID

Lucy R. Wyatt http://orcid.org/0000-0002-9483-0018
J. J. Green http://orcid.org/0000-0003-0557-3767

References

Barrick DE. 1972a. First order theory and analysis of MF/HF/VHF scatter from the sea. IEEE Trans Antennas Propag. 20:2–10.

Barrick DE. 1972b. Remote sensing of sea state by radar, In: Derr VE, editor. Remote Sensing of the Troposphere, Washington, DC GPO, Chapter 12.

Barrick DE, Weber BL. 1977. On the nonlinear theory for gravity waves on the ocean's surface. Part II: Interpretation and applications. J Phys Oceanogr. 7:11–21.

Fujii S, Heron ML, Kim K, Lai J-W, Lee S-H, Wu X, Wu X, Wyatt LR, Yang W-C. 2013. An overview of developments and applications of oceanographic radar networks in Asia and Oceania countries. Ocean Sci J. 48(1):69–97.

Green JJ, Wyatt LR. 2006. Row-action inversion of the Barrick–Weber equations. J Atmos Ocean Tech. 23:501–510.

Gurgel K-W, Antonischki G, Essen H-H, Schlick T. 1999. Wellen radar (WERA): a new ground-wave HF radar for ocean remote sensing. Coast Eng. 37:219–234.

Hanson JL, Phillips OM. 2004. Automated analysis of ocean wave directional spectra. J Atmos Ocean Tech. 18:277–293.

Harlan J, Terrill E, Hazard L, Keen C, Barrick D, Whelan C, Howden S, Kohut J. 2010. The integrated ocean observing system high-frequency radar network: status and local, region and national applications. Mar Technol Soc J. 44:122–132.

Hasselmann S, Bruning C, Hasslemann K, Heimbach P. 1996. An improved algorithm for the retrieval of ocean wave spectra from synthetic aperture radar image spectra. J Geophys Res. 101:16615–16629.

Hauser D, Kahma K, Krogstad HE, Lehner S, Monbaliu JAJ, Wyatt LR. 2005. Measuring and analyzing the directional spectra of ocean waves, vol. EUR 21367, Luxembourg Office for Official Publications of the European Communities. Luxembourg.

Lipa B, Barrick DE. 1986. Extraction of sea state from HF radar sea echo: mathematical theory and modelling. Radio Sci. 21:81–100.

Lopez G, Conley DC. 2019. Comparison of HF radar fields of directional wave spectra against in situ measurements at multiple locations. J Mar Sci Eng. 7(8):271.

Portilla J, Ocampo-Torres F, Monbalieu J. 2009. Spectral partitioning and indentification of wind-sea and swell. J Atmos Ocean Technol. 26:107–122.

Rubio A, Mader J, Corgnati L, Mantovani C, Griffa A, Novellino A, Quentin C, Wyatt L, Shulz-Stellenfleth J, Horstmann J, Lorente P, Zambianchi E, Hartnett M, Fernandes C, Zervakis V, Gorringe P, Melet A, Puillat I. 2017. HF radar activity in European coastal seas: next steps toward a pan-European HF radar network. Front Mar Sci. 4(8). https://doi.org/10.3389/fmars.2017.00008

van Vledder G, Akpinar A. 2016. Spectral partitioning and swells in the black sea. In P. Lynett (Ed.),Proceedings of the 35th International Conference on Coastal Engineering: Antalya, Turkey (Vol. 35, pp.199-212). (Proceedings of the Coastal Engineering Conference; Vol. 35).

Voorrips AC, Makin VK, Hassleman S. 1997. Assimilation of wave spectra from pitch and roll buoys in a north sea wave model. J Geophys Res. 102:5829–5849.

Waters J. 2010. Data Assimilation of Partitioned HF radar wave data into wave models, PhD thesis, University of Sheffield.

Waters J, Wyatt LR, Wolf J, Hines A. 2013. Data assimilation of partitioned HF radar wave data into wavewatch III. Ocean Model. 72:17–31.

Wyatt LR. 1990. A relaxation method for integral inversion applied to HF radar measurement of the ocean wave directional spectrum. Int J Remote Sens. 11:1481–1494.

Wyatt LR, Green JJ, Gurgel K -W, Borge JCN, Reichert K, Hessner K, Günther H, Rosenthal W, Saetra O, Reistad M. 2003. Validation and intercomparisons of wave measurements and models during the euroROSE experiments. Coast Eng. 48:1–28.

Wyatt LR, Green JJ, Middleditch A. 2011. HF radar data quality requirements for wave measurement. Coast Eng. 58:327–336.

Wyatt LR, Green JJ, Middleditch A, Moorhead MD, Howarth J, Holt M, Keogh S. 2006. Operational wave, current and wind measurements with the Pisces HF radar. IEEE J Oceanic Eng. 31:819–834.

Wyatt LR, Moorhead MD, Fairley IA. 2019. Developments in metocean HF radar technology, applications and accuracy, In: ASME 2019 38th International Conference on Ocean, Offshore and Arctic Engineering OMAE 2009 June 9–14, 2019, Glasgow, Scotland.